*Brazilian Dental Journal (2015) 26(3): 258-262*
*http://dx.doi.org/10.1590/0103-6440201300321*
ISSN 0103-6440

# Load-Application Devices: A Comparative Strain Gauge Analysis

Renato Sussumu Nishioka[1], Luis Gustavo Oliveira de Vasconcellos[1], Renata Pilli Jóias[2], Sigmar de Mello Rode[1]

[1]Department of Dental Materials and Prosthodontics, São José dos Campos Dental School, UNESP - Universidade Estadual Paulista, São José dos Campos, SP, Brazil
[2]Department of Bioscience and Oral Diagnosis, São José dos Campos Dental School, UNESP - Universidade Estadual Paulista, São José dos Campos, SP, Brazil

Correspondence: Prof. Dr. Sigmar de Mello Rode, Avenida Francisco José Longo, 777, Jd São Dimas, 12245-000 São José dos Campos, SP, Brasil. Tel: +55-12-3947-9056. e-mail:sigmarrode@uol.com.br

In view of the low loading values commonly employed in dentistry, a load-application device (LAD) was developed as option to the universal testing machine (UTM), using strain gauge analysis. The aim of this study was to develop a load-application device (LAD) and compare the LAD with the UTM apparatus under axial and non-axial loads. An external hexagonal implant was inserted into a polyurethane block and one EsthetiCone abutment was connected to the implant. A plastic prosthetic cylinder was screwed onto the abutment and a conical pattern crown was fabricated using acrylic resin. An impression was made and ten identical standard acrylic resin patterns were obtained from the crown impression, which were cast in nickel-chromium alloy (n=10). Four strain gauges were bonded diametrically around the implant. The specimens were subjected to central (C) and lateral (L) axial loads of 30 kgf, on both devices: G1: LAD/C; G2: LAD/L; G3: UTM/C; G4: UTM/L. The data (με) were statistically analyzed by repeated measures ANOVA and Tukey's test ($p<0.05$). No statistically significant difference was found between the UTM and LAD devices, regardless of the type of load. It was concluded that the LAD is a reliable alternative, which induces microstrains to implants similar to those obtained with the UTM.

Key Words: dental implants, dental prosthesis, implant-supported dental prosthesis.

## Introduction

Occlusal overload has been indicated as the primary factor for peri-implant bone resorption, implant failure and implant-supported prostheses failure (1,2). The maintenance of the bone/implant interface is particularly dependent on the control of biomechanical loads, since according to current bone physiology theories, occlusal forces affect the bone around the implant (3-5). The response to an increased mechanical stress below a certain threshold will be a strengthening of the bone by increasing the bone density or apposition of bone. On the other hand, fatigue micro-damage resulting in bone resorption may be the result of mechanical stress beyond this threshold (3-5). Moreover, during the functional load application on the implant, the direction of the forces not always coincides with its long axis. Conversely, when the occlusal force is applied on different locations and in a direction that creates leverage, it may cause stresses on the bone adjacent to the implant (4). *In vitro* (6) and *in vivo* (7) studies have revealed the negative effect of the application of non-axial loads when compared with axial loads.

Several techniques have been employed to evaluate the biomechanical loads on implants, such as photoelastic stress analysis (8-10), finite elements stress analysis (6,11), mathematical calculations (12) and strain gauge analysis (9,11,13-18).

Strain gauge analysis is a technique for measuring microstrains, which involves the use of electrical resistance or strain gauges. Strain gauges are based on the principle that certain materials undergo changes in their electrical resistivity when subjected to a force. Materials have different resistivities, which can be measured accurately at the site where the strain gage is attached, using a Wheatstone's bridge circuit (9,19). This technique has been proposed to evaluate strains in implant-supported prostheses *in vitro* (9,11,13,16-18,20), *in vivo* (15) and under static (13,16) and/or dynamic loads (21).

Strain gauge studies in implantology use low loading values varying from 20 to 300 N (8,10,11,13,18,19,22). Some works used custom-built load-application devices (8,10,11) while others used universal testing machines (13,19,22). However, the force of the universal testing machine is too great for testing small values employed in dentistry, since it is an adaptation from the engineering that requires high force. Thus, the aim of this study was to develop a load-application device (LAD) and compare the LAD with the universal testing machine (UTM) apparatus under axial and non-axial loads. The work hypotheses were: 1- both devices would produce similar magnitude of microstrain for both loading conditions; 2- the lateral load would generate greater magnitude of microstrain.

## Material and Methods

A load-application device (LAD) was developed with different magnitudes of static vertical loading (Fig. 1). The loads are applied according to the amount of weight and position of the compressor pin, varying from 5 to 40 kgf at 5 kgf intervals.

### *Preparation of the Samples*

An external implant 3.75 mm in diameter and 13 mm deep (Master screw implants; Conexão Sistemas de Prótese, São Paulo, SP, Brazil) was arranged in the middle of a polyurethane block (Polyurethane F16; Axson, Cergy, France) measuring 95 x 45 x 30 mm. EsthetiCone abutment (Conexão) was screwed onto the implant with 20 Ncm using a manual torque wrench (Conexão).

Plastic prosthetic cylinder (Conexão) was screwed onto the abutment and a conical pattern was built using acrylic resin (Duralay; Reliance Dental, Worth, IL, USA) with a 4.1 mm base, 8 mm upper platform and 8 mm high. A referential mark was made on the outermost portion of the larger base of the cone for the subsequent application of the non-axial loads.

A polyvinyl siloxane impression (Elite; Zhermack, Rovigo, Italy) was made and ten acrylic resin patterns (GC Pattern Resin; GC Europe NV, Leuven, Belgium) were obtained from the impression. The patterns were sprued, invested and cast in Co-Cr alloy (Wirobond SG; Bremen, Germany). The casts were ultrasonically cleaned, finished and polished. The fit and passivity of the superstructures were checked by direct visual examination associated with a clinical probe (23). Superstructures showing instability were excluded.

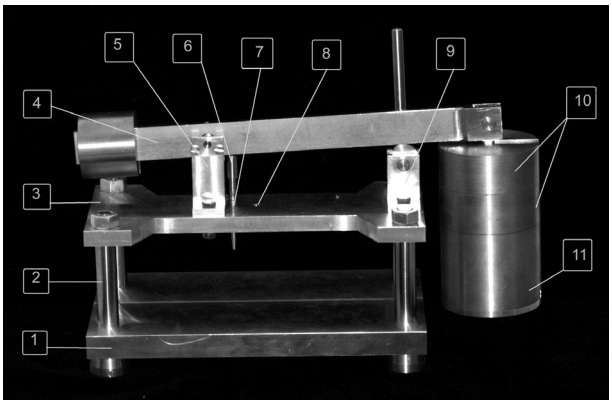


Figure 1. Load-application device (LAD) with positioned weights; 1: lower base; 2: steel rods; 3: upper base; 4: load bar; 5: load bar cradle; 6: pressure pin; 7: hole no. 1; 8: hole no. 2; 9: eccentric cradle; 10: two 1 kg weights, 11: one 2 kg weight.

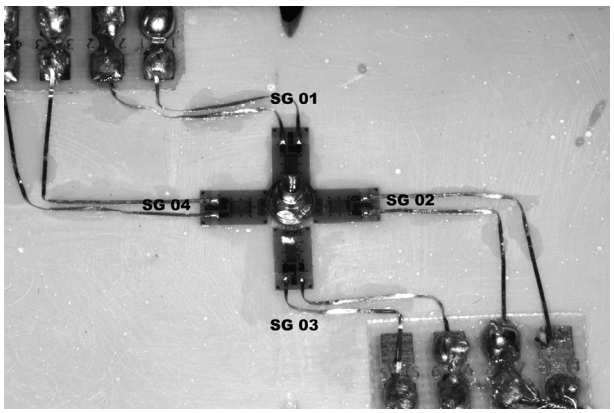


Figure 2. Experimental model and strain gauge locations.

### *Strain Gauge Analysis*

Four strain gauges (L2A-06-062LW-120; Vishay, Raleigh, NC, USA) were diametrically bonded around the implant onto the surface of the polyurethane block (Fig. 2), using methyl-2-cyanoacrylate adhesive (M-Bond 200; Vishay Measurements Group, Raleigh, NC, USA). Each strain gauge was connected separately, and the four strain gauges were arranged in series to form a one-fourth Wheatstone's bridge. The wires from the strain gauges were connected to a multichannel bridge amplifier to form one leg of the bridge. A computer (Intel 775P Pentium 4 Q6600; Acer, Miami, FL, USA) was interfaced with the bridge amplifier to record the output signal of polyurethane surface. Data acquisition system software (System 5000 Model 5100B; Vishay) was used to record the data.

### *Application of the Static Vertical Load*

Each specimen was screwed to the abutment using a torque of 10 Ncm. All of the strain gauges were zeroed and calibrated prior to each loading. Static vertical (axial) loads of 30 kgf were applied for 10 s on the entry hole of the retention screw (Fig. 3) and on the referential mark situated 4 mm from the center of the specimen (Fig. 3), which were applied using a load-application device (LAD) or the universal testing machine (DL-1000; Emic, São José dos Pinhais, PR, Brazil). The magnitude of microstrain was recorded in units of microstrain (με). This procedure was made two more times, completing three readings per loading location.

This experiment followed a factorial scheme 2x2 type. The experimental variables were device (LAD and UTM)

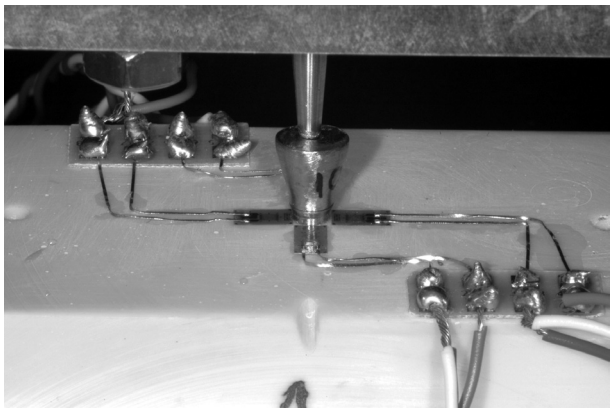

Figure 3. Application of axial load on the test specimen, using the load-application device (LAD).

and load location (center and lateral). The specimens were randomly assigned to the load location conditions.

### *Statistical Analysis*

Data obtained were submitted to statistical analysis using the following softwares: GraphPadPrism (GraphPad Software, Inc, version 4.00, 2003, La Jolla, CA, USA), MINITAB (Minitab, version 14.12, 2004, State College, PA, USA) and STATISTIX (Analytical Software Inc., version 8.0, 2003, Tallahassee, FL, USA). The statistics consisted of analysis of variance of repeated measurements for two factors (device and loading location), in which the variable loading location was considered as a repeated factor. The study of the interaction effect was conducted by graphs. Multiple comparisons among the means for the four experimental conditions were made by the Tukey's test. Significance level was set at 5%.

## Results

Table 1 shows the descriptive statistical data, analyzing the mean values of microstrain obtained with each strain gauge (SG), for the devices (LAD and UTM) at each load location (center and lateral).

The mean values of microstrain (με) of all the groups were calculated and are shown in Figure 4.

The statistical repeated measures ANOVA indicated that the load location promoted statistically significant values (p=0.0001). The interaction effect was not statistically significant, demonstrating that the device effect was similar to the one for load location.

Table 1. Values of microstrain **(με) obtained at each point where load was applied with the load-application device (LAD) and the universal testing mac**hine (UTM) on each strain gauge

| Device | Loading point | Strain gauge | Mean ± Sd |
|---|---|---|---|
| LAD | Axial | 01 | 294.2 ± 138.5 |
| | | 02 | 275.2 ± 177.5 |
| | | 03 | 281.4 ± 139.6 |
| | | 04 | 379.6 ± 246.6 |
| | Non-axial | 01 | 320.5 ± 113.7 |
| | | 02 | 735.4 ± 163.4 |
| | | 03 | 287.4 ± 129.9 |
| | | 04 | 1421.0 ± 328 |
| UTM | Axial | 01 | 486.0 ± 78.4 |
| | | 02 | 131.1 ± 86.0 |
| | | 03 | 497.8 ± 86.1 |
| | | 04 | 123.2 ± 76.7 |
| | Non-axial | 01 | 478.0 ± 55.3 |
| | | 02 | 762.2 ± 87.4 |
| | | 03 | 507.0 ± 61.5 |
| | | 04 | 1152.9 ± 112.6 |

## Discussion

The cervical region of the implant is the site where the highest stresses occur (20), regardless of the type of bone and the design of the implant (24). In this study, the strain gauges were bonded tangentially to the implant platform on the polyurethane block. This positioning of the strain gauges method has been used in previous studies (13,15-18,20). In addition, the flat surface of the polyurethane block facilitates the positioning and bonding of the strain gauges when compared with other studies, which are bonded to the implants (11), to the abutment (22) and to the metallic structures of the prosthesis (15,20).

This study compared the microstrains generated around of the implant after the application of axial (center and lateral) static loads applied by devices (LAD and UTM). According to Frost (3) and Wiskott and Belser (5), bone homeostasis occurs when the level of microstrain remains within the range from 100 to 2000 με and 50 to 1500 με, respectively. The null hypotheses were accepted, as Table 1 shows that the values of microstrain obtained after applying the 30 kgf load (center and lateral) in both load-application devices remained within the level of bone homeostasis or normal load (3,5).

In this study it was found that when the load was axial the microstrain values were smaller and equally distributed among the four strain gages. In contrast, when non axial loads were applied on the specimen, the highest microstrain values were found by the SG 4 (Fig 2) placed closest to the tip of load application, indicating that the amount of load transmitted to the bone/implant interface depends on the site where the load was applied (6-8,12). Therefore, the first work hypothesis was accepted.

Table 1 shows that the highest microstrain was obtained by the lateral load applied by both devices occurred in

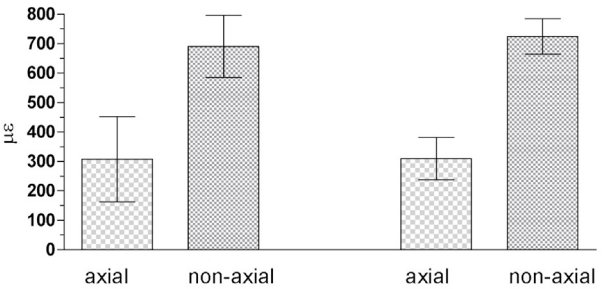


Figure 4. Mean and standard deviation of microstrain (με) for the two devices at each loading point.

the SG 4, followed by the microstrains generated in the SG 2. In other words, the lateral load caused stretching of the SG 4 and shortening of the SG 2. Similar result was reported by Hekimoglu et al. (21) on implants in occlusion with natural teeth, on implants under axial and non-axial loads and also on the cervical region of the implant during non-axial loading.

Table 2 indicates that there was no statistically significant difference between the values obtained with LAD and UTM, regardless of the type of load. This fact validates the use of the LAD for strain gauge studies. However, Table 1 showed that standard deviation of the values obtained by LAD was greater than that showed by UTM. The explanation for this fact may be due to the velocity of load application, i.e., in UTM the load is applied gradually, beginning at the moment of the tip application at 0.1 kgf until the load reaches 30 kgf. In contrast, LAD load application is quicker.

With regards to the load location (Table 2) the lateral load produced significantly higher microstrain values than those produced by central load. Based on this finding, it can be inferred that occlusal contacts positioned laterally along the axis of the implant produce higher stresses around the implant, and contribute to periimplant bone resorption. Babier and Schepers (7) analyzed the *in vivo* influence of axial and non-axial loading in bone remodeling showing that non-axial loading induces greater cell response, with strong trabecular bone anchoring, despite the presence of osteoclasts and inflammatory cells, suggesting that non-axial loads should be avoided.

Mericske-Stern et al. (25) reported maximum occlusal force of 206.1±87.6 N for the first premolars, 209.8±88.2 N for molars, and 293.2±98.3 N for second premolars in patients wearing implant-supported partial fixed prostheses. Strain gauge studies in implantology generally use low loads varying from 20 to 300 N (8-11,13,22) and other works used custom-built load-application devices (8-11). LAD can apply loads of 5 to 40 kgf at 5 kgf intervals, corresponding to loads of approximately 50 to 400 N. In this study, static axial loads of 30 kgf (±294 N) were slightly higher than those reported by Mericske et al. (25).

Limitations of the LAD must be considered in the interpretation of results. In spite of reduced cost, low purchase price and maintenance costs, easy handling, absence of electronic components and easy transportability, the device only measures static load from 5 to 40 kgf. On the other hand, UTM can be used for many other static and dynamic loading tests with low and high values. However, to increase the possibility of using the LAD, some changes should be performed, such as changes of the pin (length and diameter), pin with double or triple tip, and different scales (gf to kgf). In addition, LAD used as UTM seems to be promising for the photoelasticity analysis, since it does not prevent the transmission of the polarized light in photoelastic models.

It may be concluded that the LAD can be considered a reliable alternative, which induces microstrains similar to those obtained with the UTM regardless of the load location. The lateral load significantly increased the microstrains around the implant.


## Resumo

Considerando os valores relativamente pequenos utilizados em odontologia para os ensaios de carregamento verticais axiais, foi desenvolvido um dispositivo de aplicação de carga (DAC) para substituir a máquina de ensaios universal (EMIC). O objetivo deste estudo foi desenvolver um DAC e compará-lo com a EMIC por meio da utilização de carregamentos axiais e não-axiais. Num bloco de poliuretano foi inserido um implante hexágono externo, o qual foi conectado a um pilar protético esteticone. Sobre o pilar protético foi parafusada uma coifa plástica e um pilar cônico foi modelado em resina acrílica, que foi moldada para a obtenção de dez enceramentos iguais que foram fundidos em níquel cromo. Quatro extensômetros foram diametralmente colados ao redor do implante. Cada corpo de prova foi submetido a cargas axiais central (C) e lateral (L) de 30 kgf, em ambos os dispositivos: G1) DAC/C; G2) DAC/L; G3) EMIC/C; G4) EMIC/L. Os dados (με) foram analisados estatisticamente pelos testes de ANOVA para medidas repetidas e de Tukey ($p<0,05$). Não houve diferença estatisticamente significante entre os dispositivos DAC e EMIC, independente do tipo de carga. A aplicação de carga não-axial (NA) determinou um aumento significante de tensões ao redor do implante. Foi concluído que o DAC é uma opção confiável, a qual induz microtensão em implantes de forma semelhante à EMIC.


## References


1. Isidor F. Loss of osseointegration caused by occlusal load of oral implants. A clinical and radiographic study in monkeys. Clin Oral Implants Res 1996;7:143-152.
2. Isidor F. Histological evaluation of peri-implant bone at implants subjected to occlusal overload or plaque accumulation. Clin Oral Implants Res 1997;8:1-9.
3. Frost HM. Wolff's Law and bone's structural adaptations to mechanical usage: an overview for clinicians. Angle Orthod 1994;64:175-188.
4. Isidor F. Influence of forces on peri-implant bone. Clin Oral Implants Res 2006; 17(Suppl 2):8-18.
5. Wiskott HW, Belser UC. Lack of integration of smooth titanium surfaces: a working hypothesis based on strains generated in the surrounding bone. Clin Oral Implants Res 1999;10:429-444.
6. Barbier L, Vander Sloten J, Krzesinski G, Schepers E, Van der Perre G. Finite element analysis of non-axial versus axial loading of oral implants in the mandible of the dog. J Oral Rehabil 1998;25:847-858.
7. Barbier L, Schepers E. Adaptive bone remodeling around oral implants under axial and nonaxial loading conditions in the dog mandible. In J Oral Maxillofac Implants 1997;12:215-223.
8. Assif D, Marshak B, Horowitz A. Analysis of load transfer and stress distribution by an implant-supported fixed partial denture. J Prosthet Dent 1996;75:285-291.
9. Clelland NL, Gilat A, McGlumphy EA, Brantley WA. A photoelastic and strain gauge analysis of angled abutments for an implant system. In J Oral Maxillofac Implants 1993; 8(5):541-548.
10. Ueda C, Markarian RA, Sendyk CL, Laganá DC. Photoelastic analysis of stress distribution on parallel and angled implants after installation of fixed prostheses. Braz Oral Res 2004;18:45-52.
11. Akça K, Cehreli MC, Iplikçioglu H. A comparison of three-dimensional finite element stress analysis with *in vitro* strain gauge measurements on dental implants. Int J Prosthodont 2002;15:115-121.

12. Weinberg LA, Kruger B. A comparison of implant/prosthesis loading with four clinical variables. Int J Prosthodont 1995;8:421-433.
13. Abreu CW, Vasconcellos LGO, Balducci I, Nishioka RS. A comparative study of microstrain around three-morse taper implants with machined and plastic copings under axial loading. Braz J Oral Sci 2010;9:11-15.
14. Castilho AA, Kojima AN, Pereira SM, Vasconcellos DK, Itinoche MK, Faria R, et al.. *In vitro* evaluation of the precision of working casts for implant-supported restoration with multiple abutments. J Appl Oral Sci 2007;15:241-246.
15. Heckmann SM, Karl M, Wichmann MG, Winter W, Graef F, Taylor TD. Loading of bone surrounding implants through three-unit fixed partial denture fixation: a finite-element analysis based on *in vitro* and *in vivo* strain measurements. Clin Oral Implants Res 2006;17:345-350.
16. Nishioka RS, Nishioka LN, Abreu CW, Vasconcellos LG, Balducci I. Machined and plastic copings in three-element prostheses with different types of implant-abutment joints: a strain gauge comparative analysis. J Appl Oral Sci 2010;18:225-230.
17. Nishioka RS, Vasconcellos LG, Melo Nishioka LN. External hexagon and internal hexagon in straight and offset implant placement: strain gauge analysis. Implant Dent 2009;18:512-520.
18. Nishioka RS, Vasconcellos LG, Melo Nishioka GN. Comparative strain gauge analysis of external and internal hexagon, Morse taper, and influence of straight and offset implant configuration. Implant Dent 2011;20:e24-e32.
19. Kim WD, Jacobson Z, Nathanson D. *In vitro* stress analyses of dental implants supporting screw-retained and cement-retained prostheses. Implant Dent 1999;8:141-151.
20. Karl M, Wichmann MG, Winter W, Graef F, Taylor TD, Heckmann SM. Influence of fixation mode and superstructure span upon strain development of implant fixed partial dentures. J Prosthodont 2008;17:3-8.
21. Hekimoglu C, Anil N, Cehreli MC. Analysis of strain around endosseous dental implants opposing natural teeth or implants. J Prosthet Dent 2004;92:441-446.
22. Seong WJ, Korioth TW, Hodges JS. Experimentally induced abutment strains in three types of single-molar implant restorations. J Prosthet Dent 2000;84:318-326.
23. Kan JY, Rungcharassaeng K, Bohsali K, Goodacre CJ, Lang BR. Clinical methods for evaluating implant framework fit. J Prosthet Dent 1999;81:7-13.
24. Tada S, Stegaroiu R, Kitamura E, Miyakawa O, Kusakari H. Influence of implant design and bone quality on stress/strain distribution in bone around implants: a 3-dimensional finite element analysis. Int J Oral Maxillofac Implants 2003;18:357-368.
25. Mericske-Stern R, Assal P, Mericske E, Bürgin W. Occlusal force and oral tactile sensibility measured in partially edentulous patients with ITI implants. In J Oral Maxillofac Implants 1995;10:345-353.

*Received November 5, 2014*
*Accepted February 2, 2015*